Kaolinite and smectite dissolution rate in high molar KOH solutions at 35° and 80°C

Andreas Bauer*

Ecole Normale Supérieure, Département de Géologie, 24, rue Lhomond, 75231 Paris Cedex 05, France
BRGM, Département Géomatériaux et Géoprocédés, Avenue de Concyr, B.P. 6009, 45060 Orléans Cedex 2, France

and

Gilles Berger

UMR CNRS 5563, Université Paul-Sabatier, 38, rue des-36-ponts, 31400 Toulouse Cedex, France

Abstract—Experiments measuring kaolinite and smectite dissolution rates were carried out using batch reactors at 35° and 80°C. No potential catalysts or inhibitors were present in solution. Each reactor was charged with 1 g of clay of the $\leq 2\,\mu$m fraction and 80, 160 or 240 ml of 0.1–4 M KOH solution. An untreated but sized kaolinite from St. Austell and two treated industrial smectites were used in the experiments. One smectite is a nearly pure montmorillonite, while the second has a significant component of beidellitic charge (35%). The change in solution composition and mineralogy was monitored as a function of time. Initially, the 3 clays dissolved congruently. No new formed phases were observed by XRD and SEM during the pure dissolution stage. The kaolinite dissolution is characterized by a linear release of silica and Al as a function of the log of time. This relationship can be explained by a reaction affinity effect which is controlled by the octahedral layer dissolution. Far from equilibrium, dissolution rates are proportional to $a_{OH^-}^{0.56\pm0.12}$ at 35°C and to $a_{OH^-}^{0.81\pm0.12}$ at 80°C. The activation energy of kaolinite dissolution increases from 33 ± 8 kJ/mol in 0.1 M KOH solutions to 51 ± 8 kJ/mol in 3 M KOH solutions. In contrast to kaolinite, the smectites dissolve at much lower rates and independently of the aqueous silica or Al concentrations. The proportionality of the smectite dissolution rate constant at 35 and 80°C was $a_{OH^-}^{0.15\pm0.06}$. The activation energy of dissolution appears to be independent of pH for smectite and is found to be 52 ± 4 kJ/mol. The differences in behavior between the two kinds of minerals can be explained by structural differences. The hydrolysis of the tetrahedral and the octahedral layer appears as parallel reactions for kaolinite dissolution and as serial reactions for smectite dissolution. The rate limiting step is the dissolution of the octahedral layer in the case of kaolinite, and the tetrahedral layer in the case of smectite. © 1998 Elsevier Science Ltd. All rights reserved

INTRODUCTION

Alkaline pH solution–mineral reactions occur in a variety of geological environments as well as those where the environment has been modified by human activity in various engineering projects. Two common "engineered" high pH environments include emplaced concrete (Andersson *et al.*, 1989; Lunden and Andersson, 1989; Savage *et al.*, 1992) and alkaline flooding of sandstone reservoirs (Novosad and Novosad, 1984; Mohnot *et al.*, 1987). As an example, the pore fluids in hydraulic cement range in pH from 12.5 to 13.5, have high ionic strengths, and are dominated by Na and K in

concentration ranging from 300–4200 ppm and from 100–7500 ppm, respectively (Atkinson, 1985; Andersson *et al.*, 1989; Lunden and Andersson, 1989).

The effect of alkaline solutions on clay minerals has been the subject of study for a number of years (Velde, 1965; Eberl and Hower, 1977; Mohnot *et al.*, 1987; Chermark, 1992; Chermark, 1993; Eberl *et al.*, 1993; Huang, 1993; Bauer *et al.*, 1998). These studies focused on the formation of potassic phases such as illite and/or illite/smectite mixed layered phases. However the first stage of reaction, that is the dissolution of the initial clay, is less documented under very alkaline conditions. Accurate clay dissolution rate determinations for kaolinite are mainly far from equilibrium and for pH lower than 12.5 (May *et al.*, 1986; Carroll-Webb and Walther, 1988; Carroll and Walther, 1990; Nagy *et al.*, 1991; Wieland and Stumm, 1992; Gangor *et al.*, 1995).

*Corresponding author. Current address: Forschungszentrum Karlsruhe, Institut für Nukleare Entsorgungstechnik, PO Box 3640, D-76021 Karlsruhe, Germany.

From these studies as well as other rate measurements involving oxides and other aluminosilicates, far from equilibrium the dissolution rate can be predicted considering the mineral surface speciation and the reactivity of the different surface sites involved in the reaction (see Walther, 1996, for review). Nearer to equilibrium, the dependence of the dissolution rate on the chemical affinity of reaction has been investigated either for non-clay minerals (Rimstidt and Barnes, 1980; Berger et al., 1994a: for quartz; Berger et al., 1994b: basalt glass; Burch et al., 1993; Berger, 1995; Oelkers et al., 1994; Gautier et al., 1994: for alkali feldspar) and kaolinite under acidic conditions (Nagy et al., 1991; Oelkers et al., 1994). For aluminosilicates, chemical affinity laws have been established within the framework of the Transition State Theory (Lasaga, 1981) by considering either one activated complex (Oelkers et al., 1994) or the competition between several activated complexes (Wieland and Stumm, 1992; Berger et al., 1994b; Berger, 1995).

Bauer et al. (1998) followed the entire reaction of kaolinite in KOH solutions. They described the formation of new phases and their relation to the different liquid/solid ratios. The present experimental investigation examines the dissolution rate of kaolinite and dioctahedral smectites in high pH KOH solutions (0.1 to 4 M KOH) at temperatures of 35° and 80°C in a batch reactor. The two different silicates selected for the experiments and the choice of a closed system allows one to investigate the role of the mineral structure or composition on the rate and provide data on the chemical affinity effect. The dissolution rates were calculated from solution composition data. We also focused on the solid phase characterization prior and during the course of the experiments. All the data presented in this paper concern the pure dissolution step, prior to the formation of reaction phases. From the rate data, the temperature dependence, pH and affinity, we tried to identify the reactions which control the dissolution rates as a function of the mineral structure.

METHODOLOGY

Solid analysis methods

The starting material was characterized by X-ray diffraction (XRD), X-ray fluorescence (XRF), and scanning electron microscopy (SEM). XRD patterns were obtained on a Philips PW 1050/20 diffractometer with a stepping motor driven goniometer. Ni-filtered Cu $K\alpha_1$, α_2 radiation (fine focus tube, Philips PW 2213/20) was used. Motor displacement and intensity acquisition (Siemens proportional detector) commands were effected using a Socabim DACO system. Divergence slit, receiving slit and scatter slit were respectively 1°, 0.1 mm and 1°. Usual step size and counting times were, respectively, 0.01°2θ and 3 s. This allowed precise determinations of diffraction peak characteristics such as position and width which were effected using the decomposition program DECOMPXR (Lanson and Velde, 1992; Lanson and Besson, 1992). XRF analyses were carried out on a Philips PW 1404 analyser. SEM photographs were obtained using a JEOL GSM-6100 instrument with a KEVEX energy dispersive detector used for semi-quantitative analysis (ratio of peak height).

Starting material

Well crystallized, fine grained kaolinite (≤ 2 μm) from St. Austell (UK) was used. It is distributed under the name SUPREME and was supplied by English China Clays. SEM observations showed that the hexagonal kaolinite grains were 0.2 μm thick and varied from 0.4 to 1.0 μm in diameter. Chemical analysis by XRF determined sample composition to be 46.51% SiO_2 and 39.62% Al_2O_3, indicating that there is no excess of silica or Al in this material (Table 1). The loss of ignition (LOI) was determined gravimetrically. The presence of S and C in the starting material was checked using a LECO-125 C/S analyzer. No S or C was found.

Both samples used for the smectite experiments were dioctahedral minerals, extracted and purified from the Ibeco and Ceca industrial bentonites. The bentonites were supplied by ICO and IBECO (Germany) and BRGM (France). The ≤ 0.2 μm size fractions were isolated by sedimentation techniques (Day, 1965) and purified for organic matter by H_2O_2 treatments. The clay samples were treated at pH 3.5 to eliminate the amorphous constituents, resaturated with Na and Ca at pH 8.5 and finally washed in methanol and ethanol. The Ceca smectite is nearly a pure Na-montmorillonite, and the Ibeco clay is a Ca–smectite with a significant component of beidellitic charge (35%). The chemical analyses as determined by XRF and their structural formulae are reported in Table 1.

The starting samples were checked for purity by XRD. No constituents other than the selected minerals were indicated in the diffraction pattern, which was scanned from 2° to 70° 2θ. Their specific surface area determined by the

Table 1. Oxide composition as determined by XRF of the starting materials and the calculated structural formula. The loss of ignition (LOI) was determined gravimetrically

	SiO_2	Al_2O_3	Fe_2O_3	FeO	MgO	CaO	Na_2O	K_2O	TiO_2	MnO	P_2O_5	LOI	Total
St. Austell	46.51	39.62	–	–	–	0.11	–	0.03	–	–	–	13.74	100.01
Smectite Ceca	60.5	20.10	3.15	0.40	2.60	0.70	1.75	0.07	0.15			11.05	100
Smectite Ibeco	52.20	18.20	4.25	0.52	3.20	3.20	–	0.21	0.53	0.02		17.80	100

Kaolinite St. Austell: $Al_2Si_{1.99}Ca_{0.0025}K_{0.0016}O_5(OH)_4$.
Smectite Ceca (Wyoming-Na): $(Si_{7.98}Al_{0.02})^{IV}(Al_{3.105}Fe^{3+}_{0.3128}Fe^{2+}_{0.0443}Mg_{0.5109})^{IV}O_{22}(Na^+_{0.4475}K^+_{0.012}Ca^{2+}_{0.0984})^{CE}$.
Smectite Ibeco-Ca: $(Si_{7.65}Al_{0.35})^{IV}(Al_{2.8}Fe^{3+}_{0.47}Fe^{2+}_{0.06}Mg_{0.7})^{IV}O_{22}(K^+_{0.04}Ca^{2+}_{0.5})^{CE}$.

BET (Brunauer *et al.*, 1938) method using N_2 adsorption was found to be 11.72 m^2/g for kaolinite, 32 m^2/g for the Ceca smectite and 64 m^2/g for the Ibeco smectite. No significant change of the smectite surface area was found after a KCl treatment at neutral pH, suggesting that a possible cation exchange during the experiments will not affect the specific surface area of the samples. BET measurements of the samples altered during the dissolution stage indicate no change in the specific surface of kaolinite and the two smectites within the accuracy of the BET technique, ±10%.

Experimental protocol

The selected clay minerals were reacted at 35° and 80°C with KOH solutions ranging from 0.1 to 4 M and at various solid–solution ratios. The solutions were prepared from analytical reagent grade KOH salt, without addition of other components such as pH buffers in order to avoid

inhibition or catalysis effects. Some experiments were conducted in solutions enriched in Al or silica (5 and 15 mmol/l). For each experiment, 1 g of the sample was added to 80, 160 or 240 ml of KOH solution. Reactions were conducted in HDPE Nalgene bottles kept in ovens at 35° or 80°C with reaction times lasting up to two months. The temperature control was precise within ±3°C and accurate to ±6°C. The bottles were shaken daily (80°C) or weekly (35°C) to minimize the sedimentation of the clays and to avoid chemical gradients in solution.

The reactors and bottles were removed at specific intervals, quenched in cold water (25°C), and opened. Solution pH in the quenched bottles was measured periodically and did not vary by more than ±0.08 pH units. Subsampling was performed with great care, by removing 10 ml aliquots of a uniform suspension from the reactor vessel in order to avoid changing the total surface area to solution ratio. The extracted suspensions were filtered through a 0.1 µm Nucleopore membrane into previously cleaned polypropylene bottles. The Nucleopore membranes are made of a
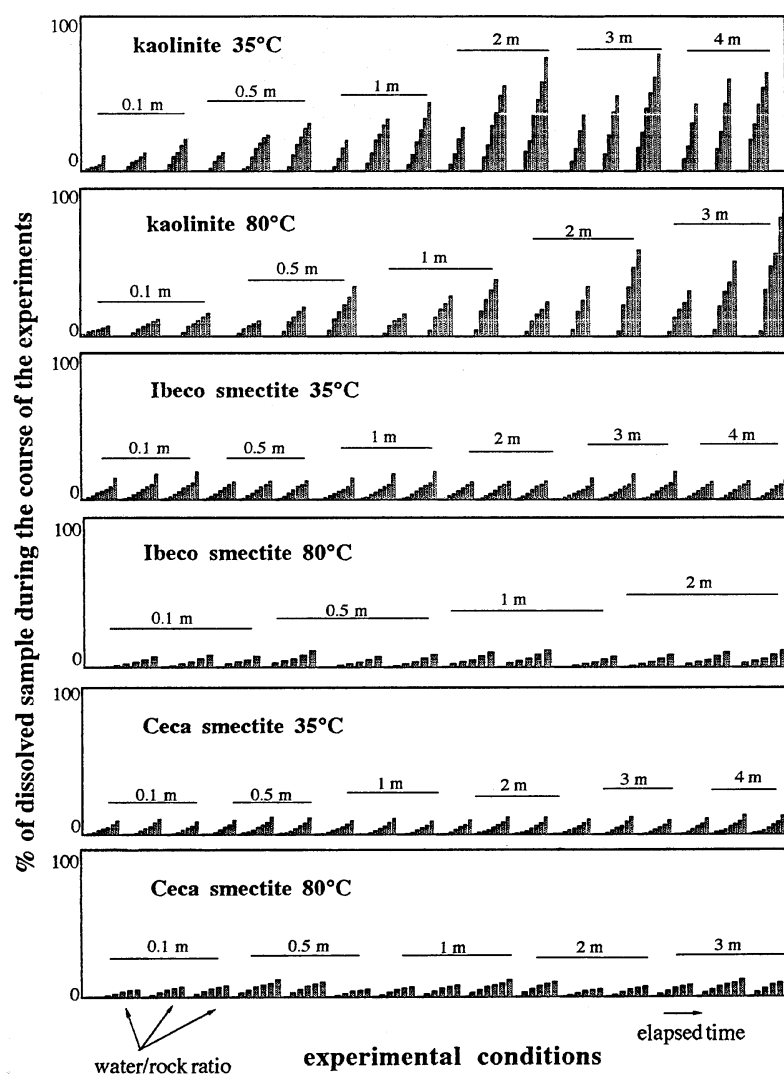

Fig. 1. Percent kaolinite and smectite dissolved as Si in solution.

polycarbonate substrate which adsorbs less than 2% of the Al in solution (Jardine *et al.*, 1986).

Concentrations of dissolved Al and silica in the filtrate were analyzed colorimetrically with an UV-visible spectrophotometer, using the Catechol violet method (Dougan and Wilson, 1974) and the Molybdate blue method (Grasshof, 1976), respectively. The uncertainty in measured Al and Si concentrations was ±3%.

The extracted solid fraction was washed with 250 ml of deionized water and divided into two parts. One part was prepared for XRD analysis (air dried and glycolated) and SEM observations. The other part was washed again in 50 ml of deionized water and dried at 60°C in reagent grade ethanol to prevent coagulation of the particles. With this material the BET surface area was measured.

Dissolution rate calculations

The clay dissolution rates were determined in each experiment from the amount of silica and aluminium released in solution between each sampling step. The first time step, before the first sampling, was not taken into account. In order to compare our data with other published studies, the rates were expressed in moles of $Si/m^2/s$. The surface area taken into account is the one determined by BET measurements, corrected by the sample mass loss resulting from the dissolution. This correction is not negligible; the mass loss of sample exceeded 75.5% of the initial mass at the end of the longer kaolinite runs as shown in Fig. 1. All the rate data presented in this paper concern the dissolution step, prior to the formation of secondary phases. Further considerations are presented in the next sections.

RESULTS AND DISCUSSION

As previously noticed, the high KOH concentrations prevented significant variations of pH during the course of the experiments. The measured concentrations of Si in solution are reported for each experiment in Tables 2–4. A typical evolution

Table 2. Summary of the measured Si concentrations in mmol/l at 35° and 80°C in the kaolinite experiments

	Kaolinite St. Austell, 35°C								
	0.1 M KOH			0.5 M KOH			1 M KOH		
days	80 ml	160 ml	240 ml	80 ml	160 ml	240 ml	80 ml	160 ml	240 ml
2	0.64	0.36	0.21	1.79	1.43	0.93	2.82	2.39	1.39
5	2.56	1.48	1.4	5.97	4.41	3.34	7.86	5.57	3.43
15	4.79	2.83	3.07	9.46	7.1	5.56	14.46	9.66	6.07
30	6.03	3.4	3.88	11.66	8.74	7.1	19.14	11.62	8.71
75	7.91	4.6	5.39		10.53	8.99		14.32	11
150	9.9	5.71	6.8		11.28	9.96		16.29	14.32
	1.5 M KOH			2 M KOH			3 M KOH		
	80 ml	160 ml	240 ml	80 ml	160 ml	240 ml	80 ml	160 ml	240 ml
2	3.79	3.11	2.25	4.71	4.46	4.11	6.07	5.36	4.93
5	9.64	6.41	5.28	10.82	8.14	6.29	14.07	11.29	8.14
15	18.73	12.26	9.05	20	14.29	11.81	25.18	18.46	13.21
30	24.11	15.69	11.92	27.36	18.25	14.96	35	23.68	16.41
75		19.27	16.31		23.57	18.81			19.69
150		23.15	22.5		26.8	23.89			24.46
	4 M KOH								
	80 ml	160 ml	240 ml						
2	7.39	6.96	6.61						
5	15.61	12.43	9.86						
15	30.21	21.29	14.04						
30	42.14	28.93	17.5						
75			20.57						
150			23.36						
	Kaolinite St.Austell, 80°C								
	0.1 M KOH			0.5 M KOH			1 M KOH		
	80 ml	160 ml	240 ml	80 ml	160 ml	240 ml	80 ml	160 ml	240 ml
0.5	1.37	1.22	0.89	1.99	1.64	1.32	2.14	2	1.46
1	2.85	2.4	2.18	5.02	4.73	3.82	7.15	6.25	5.5
1.5	3.78	3.32	2.94	7.01	6.36	5.36	10.11	8.93	8.11
2	4.52	4.17	3.59	8.72	8.14	6.89	11.74	10.79	10.14
3	5.42	4.87	4.22	10.21	9.61	8.55	14.73	13.21	12.46
5	6.73	5.65	5.02			10.9			
	2 M KOH			3 M KOH					
	80 ml	160 ml	240 ml	80 ml	160 ml	240 ml			
0.5	2.95	2.25	1.21	2.95	2.25	1.21			
1	9.86	8.21	6.93	12.5	10.01	10.24			
1.5	14.56	11.82	10.75	17.9	14.67	15.41			
2	17.94	16.57	15.07	22.29	17.79	18.16			
3	22.7	20.57	18.93	30	24.6				

Table 3. Summary of the measured Si concentrations in mmol/l at 35° and 80°C in the smectite Ibeco experiments

Smectite Ibeco, 35°C

days	0.1 M KOH			0.5 M KOH			1 M KOH		
	80 ml	160 ml	240 ml	80 ml	160 ml	240 ml	80 ml	160 ml	240 ml
2	0.69	0.34	0.23	0.85	0.42	0.28	0.95	0.48	0.32
5	1.85	0.92	0.62	2.26	1.13	0.75	2.58	1.19	0.79
10	3.60	1.93	1.29	4.61	2.26	1.51	5.18	2.59	1.73
15	6.23	2.91	1.94	6.77	3.39	2.26	7.28	3.85	2.57
20	7.78	3.89	2.59	9.29	4.64	3.10	10.71	5.36	3.57
25	9.55	4.78	3.19	11.34	5.75	3.84	12.83	6.42	4.28
30	11.62	5.81	3.87	13.97	6.92	4.61	15.22	7.63	5.09
50	19.55	9.78	6.52	23.44	11.72	7.81	25.16	12.46	8.41

days	2 M KOH			3 M KOH			4 M KOH		
	80 ml	160 ml	240 ml	80 ml	160 ml	240 ml	80 ml	160 ml	240 ml
2	1.26	0.70	0.47	0.96	0.83	0.32	0.85	0.50	0.33
5	2.88	1.60	1.02	3.18	1.68	1.06	3.02	1.43	0.95
10	5.44	2.75	1.84	6.12	2.82	2.04	5.89	2.84	1.89
15	8.29	4.11	2.74	8.70	4.25	2.90	8.93	4.47	2.98
20	10.99	5.42	3.61	11.48	5.85	3.83	12.00	6.00	4.00
25	13.73	6.67	4.50	14.19	7.09	4.73	14.17	7.08	4.72
30	16.20	8.10	5.40	16.73	8.27	5.58	17.19	8.45	5.85

Smectite Ibeco, 80°C

days	0.1 M KOH			0.5 M KOH			1 M KOH		
	80 ml	160 ml	240 ml	80 ml	160 ml	240 ml	80 ml	160 ml	240 ml
0.5	2.00	1.01	0.67	1.55	0.81	0.52	3.25	1.62	1.08
0.75	3.40	1.68	1.13	3.21	1.70	1.11	4.83	2.42	1.61
1	4.63	2.27	1.56	4.80	2.54	1.65	6.42	3.28	2.21
1.5	7.04	3.49	2.37	7.75	4.07	2.67	9.79	5.12	3.41
2	9.49	4.73	3.19	10.98	5.67	3.79		6.87	4.51

days	2 M KOH		
	80 ml	160 ml	240 ml
0.5	3.84	2.01	1.28
0.75	5.90	3.03	1.97
1	7.64	4.00	2.55
1.5	10.95	5.86	3.80
2	14.65	7.68	5.00

of the solution chemistry as a function of time for the 3 different clays is shown in Fig. 2. For the 3 materials the concentrations increase with time and were in the stoichiometric ratio of the starting clay. XRD analyses and SEM observations were carried out during the course and at the end of all the runs. No secondary minerals could be detected. Further the decomposition of the XRD patterns indicated no significant changes in the diffracting domain size distribution of kaolinite and a reduction of the coherent scattering domain size of smectites, but without illitization of the clays (Bauer and Velde, 1997; Bauer *et al.*, 1998).

From these observations it is likely that the changes of fluid chemistry correspond to a pure dissolution step. BET measurements of the solid fraction at the end of the runs indicated no change in the specific surface of the remaining samples within the ±10% accuracy of the gas adsorption technique, even when more than 75.5% of the initial mass was lost by dissolution. This suggests that the absolute surface area of the remaining sample at a given time was proportional to its mass. Thus the instantaneous dissolution rates can be easily calculated

from the solution data, by taking into account the decrease of the sample mass due to dissolution.

Kaolinite dissolution

The aqueous concentrations of Si and Al increased linearly with log (t) whatever the temperature and the KOH concentration was. This linearity with log (t) does not correlate with the loss of the sample mass. It reflects a decrease of the dissolution rate with time. Several factors influence the measured reaction rates of aluminosilicates, among them are temperature, pressure, surface area, solution composition including pH and reaction affinity. The observed linear variation of the dissolution rates with the (log) time is most likely a chemical affinity effect of the reaction.

Previous investigations on the dissolution rate of aluminosilicates versus pH far from equilibrium showed that the bulk rate is related to the surface charge of the mineral (see Walther, 1996, and references therein). This suggests a competitive effect of Si and Al detachment, depending on the specific

Table 4. Summary of the measured Si concentrations in mmol/l at 35° and 80°C in the smectite Ceca experiments

Smectite Ceca, 35°C

days	0.1 M KOH			0.5 M KOH			1 M KOH		
	80 ml	160 ml	240 ml	80 ml	160 ml	240 ml	80 ml	160 ml	240 ml
1	0.76	0.39	0.28	0.07	0.04	0.03	0.27	0.14	0.10
2	1.02	0.52	0.38	0.38	0.19	0.14	0.81	0.41	0.30
5	2.02	1.02	0.75	1.51	0.76	0.56	2.03	1.03	0.75
10	3.68	1.86	1.36	3.44	1.74	1.28	4.07	2.06	1.51
15	5.19	2.63	1.92	5.54	2.80	2.05	6.17	3.12	2.29
20	6.82	3.45	2.53	7.29	3.69	2.70	8.20	4.15	3.04
30	9.70	4.91	3.60	11.15	5.64	4.13	12.47	6.31	4.62
40	13.00	6.58	4.82	15.00	7.59	5.56			

	2 M KOH			3 M KOH			4 M KOH		
	80 ml	160 ml	240 ml	80 ml	160 ml	240 ml	80 ml	160 ml	240 ml
1	0.37	0.19	0.14	2.13	1.08	0.79	1.39	0.71	0.52
2	0.73	0.37	0.27	2.71	1.37	1.00	1.85	0.94	0.69
5	2.06	1.04	0.76	4.11	2.08	1.52	3.12	1.58	1.16
10	4.51	2.28	1.67	6.62	3.35	2.46	5.67	2.87	2.10
15	6.87	3.48	2.55	9.01	4.56	3.34	8.33	4.22	3.09
20	9.19	4.65	3.41	11.56	5.85	4.29	10.83	5.48	4.02
30	13.80	6.98	5.11	16.59	8.39	6.15	15.99	8.09	5.93

Smectite Ceca, 80°C

	0.1 M KOH			0.5 M KOH			1 M KOH		
	80 ml	160 ml	240 ml	80 ml	160 ml	240 ml	80 ml	160 ml	240 ml
0.50	1.80	0.90	0.60	2.40	1.19	0.80	3.20	1.61	1.07
1.00	3.84	1.92	1.28	5.14	2.51	1.68	6.06	3.03	2.02
1.50	6.03	3.03	2.02	7.69	3.80	2.54	8.88	4.50	3.02
1.75	7.11	3.52	2.35	9.21	4.58	3.06	10.27	5.25	3.52
2.00	8.02	3.99	2.66	10.40	5.15	3.44	11.74	5.99	4.02

	2 M KOH			3 M KOH		
	80 ml	160 ml	240 ml	80 ml	160 ml	240 ml
0.50	4.17	2.07	1.38	4.84	2.45	1.63
1.00	7.37	3.68	2.45	7.97	3.98	2.76
1.50	10.52	5.28	3.52	11.16	5.55	3.94
1.75	12.21	6.04	4.04	12.93	6.46	4.51
2.00	13.87	6.90	4.61	14.70	7.39	5.09

charge of the relevant surface sites. In case of kaolinite in basic solutions, Xie and Walther (1992) and Walther (1996) proposed that the $\equiv Si-O^-$ surface groups will account for most of the surface charge below pH 11, while the $=Al-O^-$ surface groups will begin to dominate surface charge above pH 11. At the high pH of the solutions in our experiments, it is likely that the initial dissolution of kaolinite is dominated by the detachment of Al. This assumption is supported by the results of experiments conducted in solutions enriched in either silica or Al. Figure 3 shows that the initial kaolinite dissolution is inhibited in presence of aqueous Al, but not Si. A preferential Al release cannot be observed in our experiments given the great amount of dissolved material (Fig. 1).

Nearer to equilibrium, the dependence of dissolution rate on the chemical affinity can be derived within the framework of the Transition State Theory (Lasaga, 1981 and references therein). However, the application of this concept from homogeneous to heterogeneous kinetics (involving serial reactions) requires that the elementary molecular reactions which control the overall rate are clearly identified. If only one elementary reaction is assumed to control the overall rate and if the activated complex is assumed to be the same for dissolution and precipitation, the rate–affinity relation takes the form of a first order law by applying the method of detailed balancing between the forward and reverse reactions as given by equation (1):

$$rate = k_+ \times (1 - Q/K) \qquad (1)$$

where *rate* denotes the overall dissolution rate (mol/surface/time), k_+ is the rate constant for dissolution at a given temperature and pH, Q and K stand for the activity quotient and the equilibrium constant of the bulk reaction, respectively, and Q/K is the degree of saturation of the solution with respect to the dissolving phase.

Such a simple relation has been used for the dissolution of simple oxides like quartz (Rimstidt and Barnes, 1980; Berger *et al.*, 1994a). In the case of multiple oxides, this relation is much more complex, mainly because the chemistry of the rate-limiting step differs from that of the bulk reaction. In the case of feldspars for example, chemical affinity laws have been established by considering either one acti-
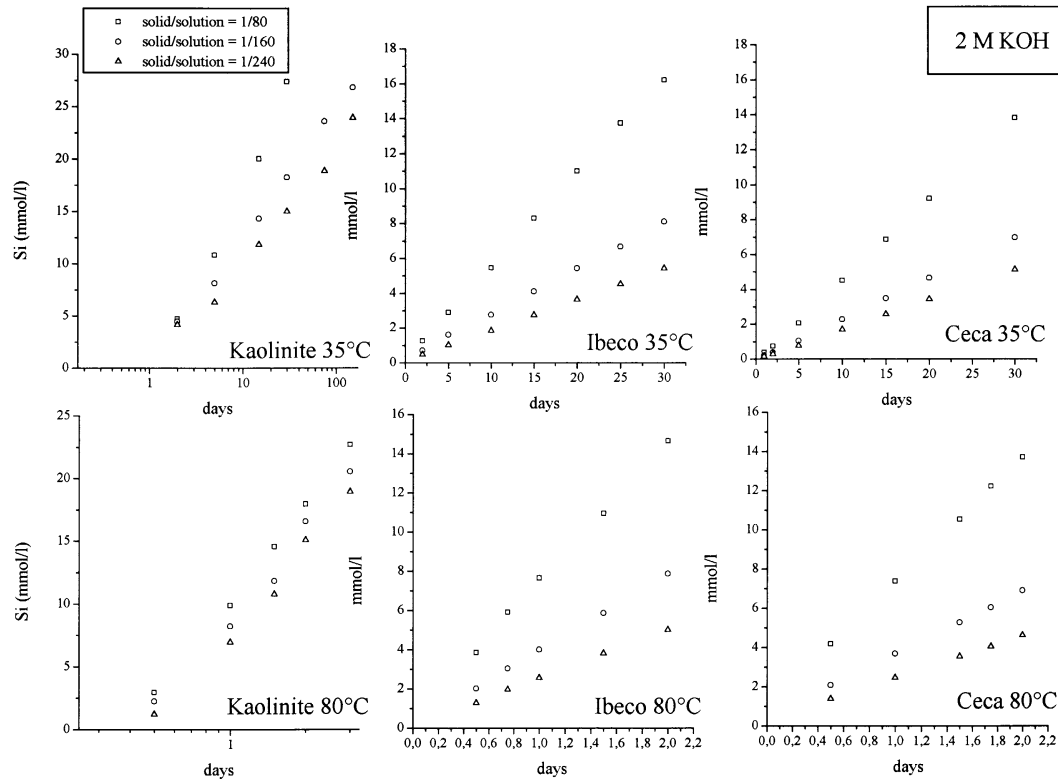
Fig. 2. Evolution of the Si concentrations in solution as a function of time for the 3 different clays in a 2 M KOH solution at 35° and 80°C. The time scale for the kaolinite experiments is logarithmic.

vated complex (Oelkers *et al.*, 1994) or the competition between several activated complexes (Berger *et al.*, 1994b; Berger, 1995).

In order to progress in the comprehension of the controlling mechanism in kaolinite dissolution, an attempt was made to find a single rate/fluid composition relation which will fit all the data. If such an internally consistent relation exists, independently of the experimental conditions, it is likely that it

describes the (or succession of) reaction(s) which controls the dissolution. In order to compare data from different conditions the ratio r/r_0 was used where r denotes the measured dissolution rate at each time and r_0 is the rate far from equilibrium at the same temperature and KOH conditions. This was carried out as follows:

— The values of r_0, the rate in Al and Si-free solutions (k_+ in equation (1)), were estimated at
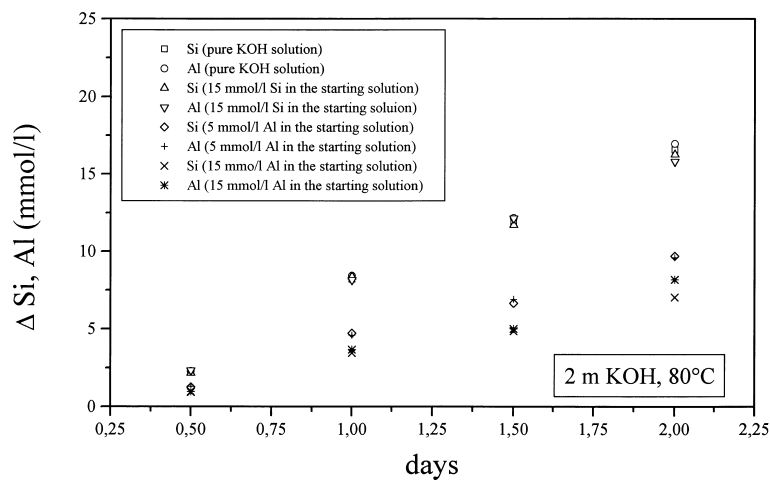
Fig. 3. Si and Al release in a 2 M KOH solution at 80°C. The diagram shows the evolution of the ΔSi and ΔAl (element$_{measured}$–element$_{in\ starting\ solution}$) concentrations in mmol/l for the pure KOH solution and for solutions enriched in Al (5 or 15 mmol/l) or Si 15 mmol/l.
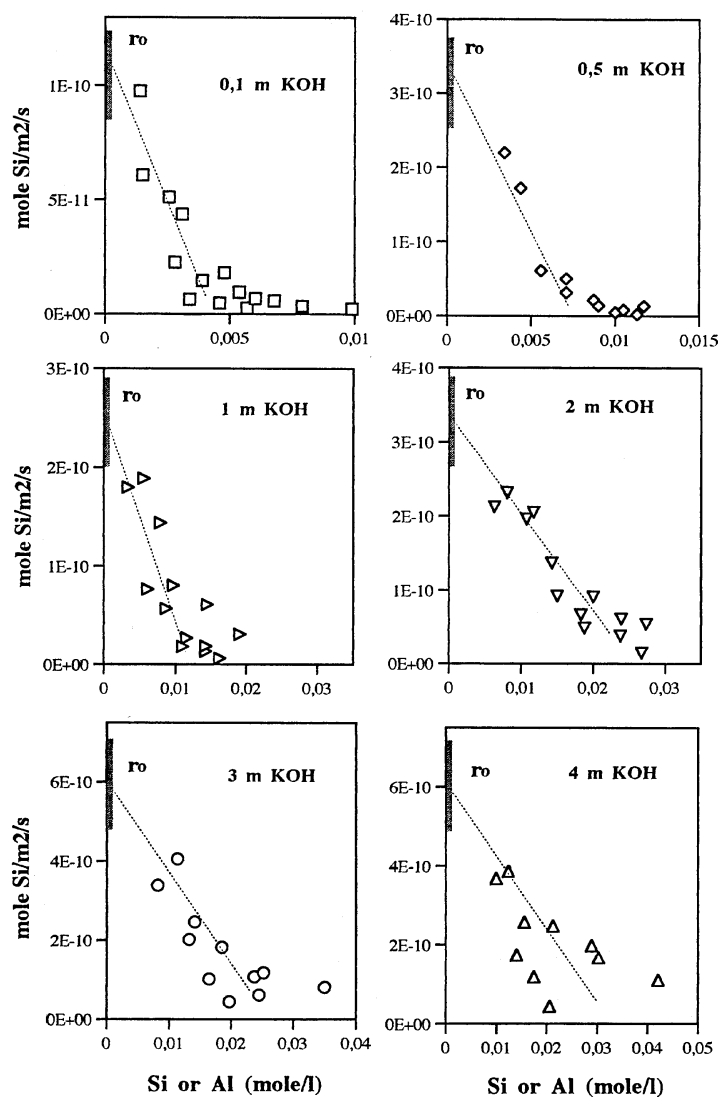
Fig. 4. Dependence of the kaolinite dissolution rate at 35°C on the aqueous Al or Si concentrations; r_0, the rate in Al- and Si-free solutions, is estimated at $\pm 20\%$ by assuming a linear relation between the rate and the concentrations in the first stages of reaction (dashed lines).

Table 5. Dissolution rate constant (r_0) of kaolinite and smectites. The accuracy of the determination is estimated to be within 20% for kaolinite and 10% for the smectites

KOH (M)	*in situ* initial pH	Rate constant (mol Si/m²/s)		
		kaolinite	Ibeco smec.	Ceca smec.
35°C				
0.1	12.56	$1.1\ 10^{-10}$	$6.0\ 10^{-12}$	$9.8\ 10^{-12}$
0.5	13.18	$3.0\ 10^{-10}$	$7.5\ 10^{-12}$	$1.2\ 10^{-11}$
1.0	13.44	$3.0\ 10^{-10}$	$8.0\ 10^{-12}$	$1.3\ 10^{-11}$
2.0	13.69	$3.5\ 10^{-10}$	$8.5\ 10^{-12}$	$1.5\ 10^{-11}$
3.0	13.86	$6.0\ 10^{-10}$	$8.7\ 10^{-12}$	$1.6\ 10^{-11}$
4.0	13.92	$6.0\ 10^{-10}$	$9.0\ 10^{-12}$	$1.7\ 10^{-11}$
80°C				
0.1	11.47	$0.7\ 10^{-9}$	$7.5\ 10^{-11}$	$1.3\ 10^{-10}$
0.5	12.09	$1.9\ 10^{-9}$	$9.7\ 10^{-11}$	$1.7\ 10^{-10}$
1.0	12.35	$3.0\ 10^{-9}$	$1.0\ 10^{-10}$	$1.8\ 10^{-10}$
2.0	12.61	$5.0\ 10^{-9}$	$1.2\ 10^{-10}$	$2.1\ 10^{-10}$
3.0	12.74	$7.0\ 10^{-9}$		$2.3\ 10^{-10}$
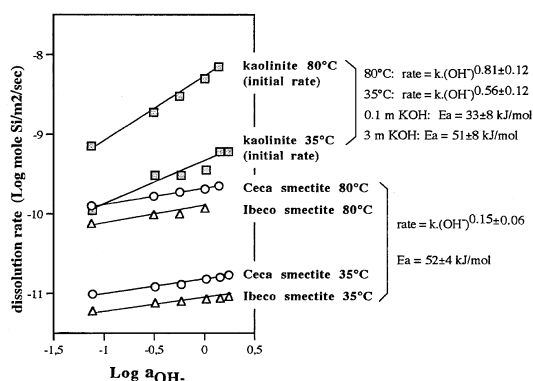
Fig. 5. Initial dissolution rate (r_0) of kaolinite and smectites at 35° and 80°C vs the activity of OH^- in solution. The proportionality of r_0 to $a_{OH^-}^{0.56 \pm 0.12}$ is at 35°C and $a_{OH^-}^{0.81 \pm 0.12}$ at 80°C The activation energy (E_a) of kaolinite dissolution increases from 33 ± 8 kJ/mol in 0.1 M KOH

$\pm 20\%$ for each temperature and KOH molarity by extrapolating the observed rate–concentration relation to zero solution concentration. A linear rate dependence was assumed in the first stages of reaction on the aqueous Al or Si concentrations. Examples are shown for 35°C in Fig. 4 and the values of r_0 are reported in Table 5.

— The pH and activities of water and aqueous species, as well as the saturation index of kaolinite, were calculated at *in situ* conditions by using the EQ3/6 software package (Wolery, 1983; Wolery and Daveller, 1990) and the SUPCRT92 database (Johnson *et al.*, 1992). The *in situ* pH was determined by calculating the charge balance on H^+. That the presence of small amounts of other cations does not change the pH calculations, given the high K concentrations was checked.

Rate constants

The kaolinite dissolution rate far from equilibrium depends on temperature and pH. From data reported in Table 5, it was found that there is a proportionality of r_0 to $a_{OH^-}^{0.56 \pm 0.12}$ at 35°C and to $a_{OH^-}^{0.81 \pm 0.12}$ at 80°C, by plotting $\log (r_0)$ vs $\log (a_{OH^-})$ or pH (Fig. 5). According to Walther (1996) the increase of rate with pH reflects an equivalent increase of the surface charge. It can also be related to the adsorption of OH^- as proposed by Xiao and Lasaga (1996) for the quartz dissolution in basic media. The pH dependence is not the same at 35° and 80°C suggesting a small pH effect on the activation energy of kaolinite dissolution. However, the calculated *in situ* pH range is not the same for the two temperatures, mainly because of the change of the water dissociation constant with temperature. At pH 12.5, which is a common pH value for the both sets of experiments, the activation energy of kaolinite dissolution is 67 ± 8 kJ/mol. On the other hand, at a given OH^- activity, the activation energy of kaolinite dissolution increases from 33 ± 8 kJ/mol in 0.1 M KOH solutions to 51 ± 8 kJ/mol in 3 M KOH solutions. These last values are more consistent with the assumed molecular reaction which implies adsorption of OH^-. It was also found that rates far from equilibrium were two order of magnitudes higher than those predicted from Carroll and Walther (1990) for the present experimental conditions. This difference can be explained by a reaction affinity effect on the Carroll and Walthers rates in basic solutions, as observed in the present study.
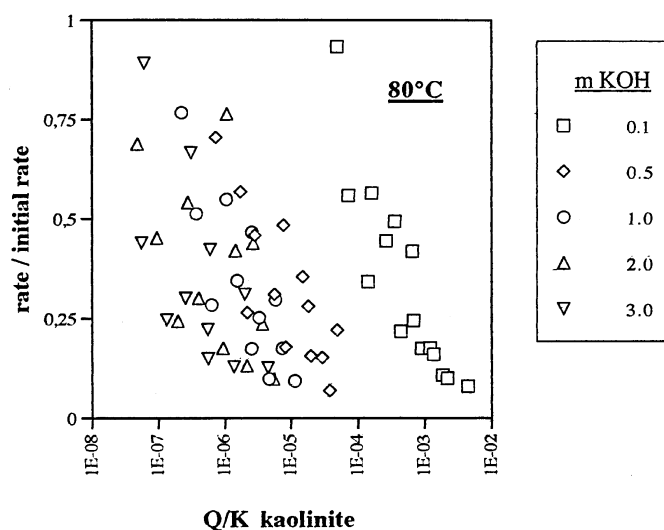

Fig. 6. Kaolinite dissolution rates at 80°C vs the saturation index of the solution. There is not a single relation which fits the data.
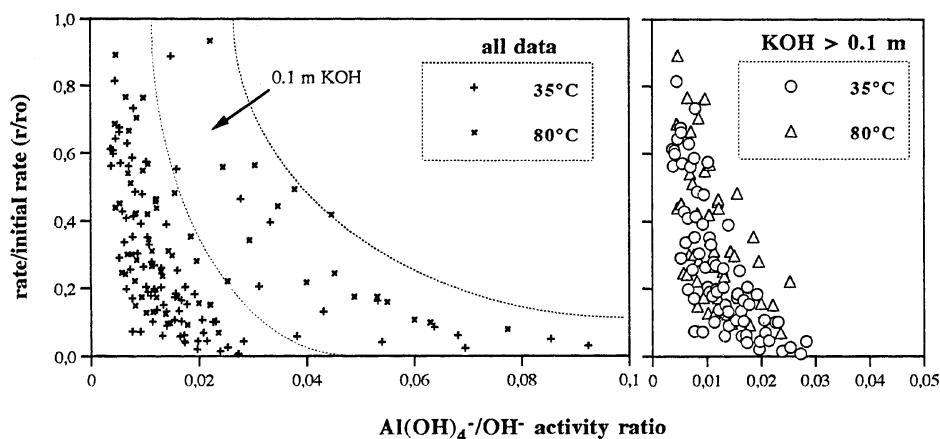
Fig. 7. Dependence of the kaolinite dissolution rates at 35° and 80°C on the $Al(OH)_4^-/OH^-$ activity ratio. A single relation seems to fit all the data.

Effect of solution composition

As for other aluminosilicates, preliminary thermodynamic calculations showed that the measured kaolinite dissolution rates cannot be easily related to the chemical affinity of the overall reaction. The speciation calculations showed that the solutions were always largely undersaturated with respect to kaolinite. There was not a unique relation between the rate decrease and the calculated saturation index either. For example, the dependence of the rates at 80°C on $Q/K_{kaolinite}$ is presented in Fig. 6. On the other hand, a single relation between r/r_0 and the $Al(OH)_4^-/OH^-$ activity ratio seems to fit all the data, excepting the rates at lower pH (0.1 M KOH). This relation is shown in Fig. 7.

This rate dependence on solution composition can be related to the hydrolysis of the octahedral layer. Aluminum is linked together to bonding oxygens with Si and to OH groups. Detachment of an aluminum atom from the octahedral layer (which is assumed more reactive that Si because it is more highly charged at the surface) can be described as follows (the surface charge is not represented here):

$$O_{3/2}{\equiv}Si{-}O_{2/2}{-}Al{=}(OH)_{4/2} + H_2O + OH^- \longrightarrow$$

$$O_{3/2}{\equiv}Si{-}OH + Al(OH)_4^- \qquad (2)$$
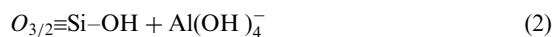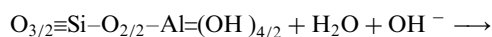
Using the description given by Hiemstra and Van Riemsdijk (1990) for the dissolution of metal (hydr) oxides, the partial hydrolysis of Si which results from the dissolution of the octahedral layer most likely promotes the dissolution of the tetrahedral layer, this later step being non rate-limiting. If one assumes equation (2) to be reversible and rate-limiting, a "contextual" solubility product can be defined and the bulk dissolution rate at a given temperature becomes a function of the $Al(OH)_4^-/(OH^-{\cdot}H_2O)$ activity ratio according to equation (1). However, because the variation of the water activity with KOH concentration was limited within the

0.85–1 interval, the rate is roughly a function of $Al(OH)_4^-/(OH^-)$. This is exactly what is shown in Fig. 7 for KOH molarities higher than 0.1 M. At lower pH, the dispersion of the data suggests a change in the controlling reaction (hydrolysis of tetrahedral layer?). The fact that a single relation accounts for the dissolution at two temperatures also suggests that the "solubility" of the octahedral layer is weakly temperature dependent.

Smectite dissolution

In contrast to kaolinite, the concentrations of Si and Al in solution increased linearly with time. For a given temperature and KOH concentration, the calculated dissolution rates are constant with time and independent of the solid–solution ratio suggesting no chemical affinity effect. The absence of a chemical affinity effect suggests that the dissolution of smectites proceeded far from equilibrium, and that the measured rates correspond to the rate constants. The numerical values of the smectite dissolution rate constants are reported in Table 5 and are compared with those of kaolinite in Fig. 5. When plotting $\log(rate)$ vs $\log(a_{OH^-})$, the same proportionality of the smectite dissolution rate constant to $a_{OH^-}^{0.15 \pm 0.06}$ is found at 35° and 80°C. The activation energy of smectite dissolution appears independent of pH and is found to be 65 ± 4 kJ/mol at pH 12.5 or 52 ± 4 kJ/mol at a given OH^- activity.

These differences with kaolinite can be explained by structural considerations. As discussed above, it is likely that the Al sites are more reactive than the Si sites under the experimental conditions. But in contrast with kaolinite, each aluminous octahedral layer in smectites is bonded to two silica rich tetrahedral layers. The accessibility of water to the Al–O or Al–OH bonds is limited to the edges of the par-

ticles until the tetrahedral layers are dissolved. If one assumes that the surface of the edges of the particles is negligible with respect to the surface of the basal planes, one can consider the hydrolysis of the octahedral and tetrahedral layer as serial reactions. This implies that the bulk rate is controlled by the slower step, the dissolution of the tetrahedral layer. This assumption is supported by several observations:

— the smectite dissolution rate constants are one to two orders of a magnitude lower than for kaolinite;

— the absence of a chemical affinity effect is consistent with the high solubility of the silicic phases in this pH range;

— the slight pH dependence.

This last point can be discussed by comparing the dissolution rate of quartz and corundum as analogues of the Si–O and Al–O bonds. Data reported in Walther (1996) show that the dissolution of corundum is more pH-dependent in alkaline solutions than the dissolution of quartz. Further, the raw data also show that the pH dependence of the quartz dissolution rate decreases above pH 10. The slight pH dependence of smectite dissolution found in the present study at high pH, when compared to the higher pH values dependence of kaolinite dissolution under the same conditions, seem to correlate the observed differences between quartz and corundum dissolution rates in basic media.

The two smectites used in the present study exhibit the same kinetic features, but their absolute rates differ by a factor of two. Welch and Ullman (1996) observed a dependence of the dissolution rate constant of feldspars at acidic conditions on the Al concentrations of the minerals. A similar effect is likely for other aluminosilicates provided that the Al surface sites are more reactive than the Si sites. In the present study, the tetrahedral layers are more Al-substituted in the Ibeco smectite than in the Ceca smectite but in the both cases the Al/Si ratio is very low: 0.046 (smectite Ibeco) and 0.0025 (smectite Ceca), respectively. Further, the Ibeco smectite which has more tetrahedral Al presents the slower rate. The authors do not believe that such a small Al content in the tetrahedral layer influences the dissolution rate constant. On the other hand, the observed rate difference corresponds exactly to the difference in the surface area as determined by the BET method. This raises the question of the surface area values used in the rate calculations. It is assumed that the reactive surface areas during dissolution were the same as those measured by gas adsorption on the dry material. But it is questionable if the accessibility of gas and water is equivalent, in particular on the interlayer planes within the particles. This problem has not been solved and is an open question.

CONCLUSION

The dissolution rate of kaolinite and two dioctahedral smectites was measured in batch reactors at $35°$ and $80°C$ in KOH solutions, from the silica and Al released in solution. The solid phase characterization prior and during the course of the experiments were also examined. All the data presented in this paper concern the pure dissolution step.

The kaolinite dissolution is characterized by a linear release of silica and Al with (log) time. At both temperatures a correlation is found between the instantaneous rate and the $Al(OH)_4^-/OH^-$ activity ratio. This apparent relationship is explained by an affinity effect of the octahedral layer dissolution. Far from equilibrium, the rates are proportional to $a_{OH^-}^{0.56 \pm 0.12}$ at $35°C$ and to $a_{OH^-}^{0.81 \pm 0.12}$ at $80°C$. At constant OH^- activity, the activation energy of kaolinite dissolution increases from 33 ± 8 kJ/mol in 0.1 M KOH solutions to 51 ± 8 kJ/mol in 3 M KOH solutions.

In contrast to kaolinite, the smectites dissolve at much lower rates and independently of the aqueous silica or Al concentrations. No chemical affinity effect is observed. The same proportionality of the smectites dissolution rate constant to $a_{OH^-}^{0.15 \pm 0.06}$ was found at $35°$ and $80°C$. The activation energy of dissolution appears independent of pH and is found to be 52 ± 4 kJ/mol at a given OH^- activity.

The differences in behavior between the two different kinds of minerals is explained by structural differences. The hydrolysis of the tetrahedral and octahedral layers appear as parallel reactions for kaolinite dissolution and serial reactions for the smectite dissolution. The limiting step is the dissolution of the octahedral layer in the case of kaolinite, and the tetrahedral layer in the case of smectite.

REFERENCES

Andersson K., Allard B., Bengtsson M. and Magnusson B. (1989) Chemical composition of cement pore waters. *Cement Concrete Res.* **19**, 327–332.

Atkinson A. (1985) The time dependence of the pH within a repository for radioactive waste disposal. *AERE R11 777*. HMSO, London.

Bauer A. and Velde B. (1997) Smectite transformation in KOH solutions. *Abstracts of the Int. Clay Conf.* 97, Ottawa, Canada.

Bauer A., Velde B., Berger G. (1998) Kaolinite transformation in high molar KOH solutions, *Appl. Geochem.*, in press.

Berger G., (1995) The dissolution rate of sanidine at near neutral pH as a function of silica activity at 100, 200, and 300°C. In *Water-Rock-Interaction*, ed. Y. K. Kharaka and O. Chudaev, pp. 141–144. Balkema, Rotterdam.

Berger G., Cadore E., Schott J. and Dove P. (1994a) Dissolution rate of quartz in lead and sodium electrolyte solutions. Effect of the nature of surface complexes and reaction affinity. *Geochim. Cosmochim. Acta* **58**, 541–551.

Berger G., Claparols C., Guy C. and Daux V. (1994b) Dissolution rate of a basalt glass in silica rich solutions: Implications for long-term alteration. *Geochim. Cosmochim. Acta* **58**, 4875–4886.

Brunauer S., Emmett P. H. and Teller E. (1938) Adsorption of gases in multimolecular layers. *J. Am. Chem. Soc.* **60**, 309–319.

Burch T. E., Nagy K. L. and Lasaga A. C. (1993) Free energy dependence of albite dissolution kinetics at 80°C, pH 8.8. *Chem. Geol.* **105**, 137–162.

Carroll-Webb S. and Walther J. V. (1988) A surface complex reaction model for the pH-dependence of corundum and kaolinite dissolution. *Geochim. Cosmochim. Acta* **52**, 2609–2623.

Carroll S. A. and Walther J. A. (1990) Kaolinite dissolution at 25°, 60° and 80°C. *Am. J. Sci.* **290**, 797–810.

Chermark J. A. (1992) Low temperature experimental investigation of the effect of high pH NaOH solutions on the Opalinus shale, Switzerland. *Clays Clay Minerals* **40**, 650–658.

Chermark J. A. (1993) Low temperature investigation on the effect of high pH KOH on the Opalinius Shale Switzerland. *Clays Clay Minerals* **41**, 365–372.

Day P. R. (1965) Particle fractionation and particle size analysis. In *Methods of Soil Analysis*, ed. C. A. Black, pp. 545–567. Am. Soc. Agron. Inc.

Dougan W. K. and Wilson A. L. (1974) The absorptiometric determination of Al in water. A comparison of some chromogenic reagents and the development of an improved method. *Analyst* **99**, 413–430.

Eberl D. D. and Hower J. (1977) The hydrothermal transformation of sodium and potassium smectite into mixed layer clays. *Clays Clay Minerals* **25**, 215–227.

Eberl D. D., Velde B. and McCormick T. (1993) Synthesis of illite–smectite from smectite at earth surface temperatures and high pH. *Clay Minerals* **28**, 49–60.

Gangor J., Mogollon J. L. and Lasaga A. C. (1995) The effect of pH on kaolinite dissolution rates and on activation energy. *Geochim. Cosmochim. Acta* **59**, 1037–1052.

Gautier J. M., Oelkers E. H. and Schott J. (1994) Experimental study of K-feldspar dissolution rates as a function of chemical affinity at 150°C and pH 9. *Geochim. Cosmochim. Acta* **58**, 4549–4560.

Grasshof K. (1976) *Methods of seawater analysis*. Springer Verlag.

Hiemstra T. and Van Riemsdijk W. H. (1990) Multiple activated complex dissolution of metal (hydr)oxides. *J. Colloid Interf. Sci.* **6**, 132–150.

Huang W. J. (1993) The formation of illitic clays from kaolinite in KOH solution from 225°C to 350°C. *Clays Clay Minerals* **6**, 645–654.

Jardine P. M., Zelaszny L. W. and Evans A. (1986) Solution aluminium anomalies resulting from various filtering materials. *Soil Sci. Am.* **50**, 891–894.

Johnson J. W., Oelkers E. H. and Helgeson H. C. (1992) SUPCRT92 a software package for calculating the standard thermodynamic properties of minerals, gases, aqueous species and reactions from 1 to 500 bar and 0 to 1000°C. *Comput. Geosci.* **8**, 889–947.

Lanson B. and Besson G. (1992) Characterisation of the end of smectite to illite transformation: Decomposition of X-ray patterns. *Clays Clay Minerals* **40**, 40–52.

Lanson B. and Velde B. (1992) Decomposition of X-ray diffraction patterns; a convenient way to describe complex diagenetic evolutions. *Clays Clay Minerals* **40**, 629–643.

Lasaga A. C. (1981) Transition State Theory. In *Kinetics of Geochemical Process*, ed A. C. Lasaga and R. J. Kirkpatrick, pp. 169–195. *Rev. Mineral.* 8, Mineral Soc. Am., Washington, DC.

Lunden I. and Andersson K. (1989) Modelling the mixing of cement pore water and groundwater using the PHREEQE code. *Mater. Res. Soc. Symp. Proc.* **127**, 949–956.

May H. M., Kinniburgh D. G., Melmke P. A. and Jackson M. L. (1986) Aqueous dissolution, solubilities and thermodynamic stabilities of common aluminosilicate clay minerals: Kaolinite and smectites. *Geochim. Cosmochim. Acta* **50**, 1667–1677.

Mohnot S. M., Bae J. H. and Foley W. L. (1987) A study of alkali/mineral reactions. *SPE Reservoir Engng.* Nov., 653–663.

Nagy K. L., Blum A. E. and Lasaga A. C. (1991) Dissolution and precipitation kinetics of kaolinite at 80°C and pH 3. *Am. J. Sci.* **291**, 649–686.

Novosad, Z. and Novosad, J. (1984) Determination of alkalinity losses resulting from hydrogen ion exchange in alkaline flooding. *SPE of AIME*, 49–52.

Oelkers E., Schott J. and Dedival J. L. (1994) The effect of aluminium, pH, and chemical affinity on the rates of aluminosilicate dissolution reactions. *Geochim. Cosmochim. Acta* **58**, 2011–2024.

Rimstidt J. D. and Barnes H. L. (1980) The kinetics of silica–water interactions. *Geochim. Cosmochim. Acta* **44**, 1683–1700.

Savage D., Bateman K., Hill P., Hughes C., Milodowski A., Pearce J., Rae E. and Rochelle C. (1992) Rate and mechanism of the reaction of silicates with cement pore waters. *Appl. Clay Sci.* **7**, 33–45.

Velde B. (1965) Experimental determination of muscovite polymorph stabilities. *Am. Min.* **50**, 436–449.

Walther J. (1996) Relation between rates of aluminosilicate mineral dissolution, pH, temperature, and surface charge. *Am. J. Sci.* **296**, 693–728.

Welch S. A. and Ullman W. J. (1996) Feldspar dissolution in acidic and organic solutions: Compositional and pH dependence of dissolution rate. *Geochim. Cosmochim. Acta* **60**, 2939–2948.

Wieland E. and Stumm W. (1992) Dissolution kinetics of kaolinite in acid aqueous solutions at 25°C. *Geochim. Cosmochim. Acta* **56**, 3339–3355.

Wolery T. J. (1983) EQ3NR, a computer program for geochemical aqueous speciation-solubility calculations: User's guide and documentation. Lawrence Livermore Nat. Lab., Livermore, CA, UCRL-53414-report.

Wolery T. J. and Daveller S. A. (1990) EQ6, a computer program for reaction path modelling of aqueous geochemical systems: User's guide and documentation. Lawrence Livermore Nat. Lab., Livermore, CA, UCRL-MA-110662.

Xiao Y. and Lasaga A. C. (1996) Ab-initio quantum mechanical studies of the kinetics and mechanisms of quartz dissolution: OH^- catalysis. *Geochim. Cosmochim. Acta* **60**, 2283–2295.

Xie Z. and Walther J. V. (1992) Incongruent dissolution and surface area of kaolinite. *Geochim. Cosmochim. Acta* **56**, 3357–3363.